

Thermodynamic Evaluation of Integrated Heat Pipe Reformer SOFC System

S. Herrmann^a, M. Jimenez Arreola^a, M. Gaderer^a, and H. Spliethoff^{a,b}

^a Institute for Energy Systems, Munich Technical University, Garching 85747, Germany

^b ZAE Bayern, Garching 85747, Germany

Optimized integration of SOFC and gasification offers the potential for highly efficient electricity generation from renewable solid feedstock. In the presented integration approach heat pipes are used to transport heat from the SOFC to a biomass gasifier. Combined with further system optimization measures an electrical efficiency of 61.2% is achieved.

Introduction

Every increase in power generation efficiency leads to a potential for lower carbon dioxide emissions from power generation. Fuel cells, and more specific Solid Oxide Fuel Cells (SOFC), are the most efficient power generation devices available. Depending on operating parameters, such as temperature, pressure and fuel utilization, SOFC can achieve an exergy efficiency of more than 90% (1), far beyond any other present day technology. However, finally it greatly depends on the design of the surrounding system which share of this efficiency can be exploited. Furthermore, the type of fuel fed to the SOFC decides, if the SOFC system can be regarded as a “green” technology yielding a positive, neutral, or even a negative balance with regards to CO₂ emissions. In view of climate change in the longer term CO₂ neutral systems will be obligatory and maybe even CO₂ negative systems will be necessary to reverse the global temperature increase.

For this purpose renewable feedstock is necessary for SOFC based power systems. This can be achieved using gaseous fuel from either biological digestion or thermochemical gas generation. The latter offers a much wider range of potential feedstock, such as waste or wood, which is not degradable by digestion with present day technology. Furthermore, the operating temperatures of gasifiers, which are typically used for thermochemical conversion of biomass to gaseous fuels, and SOFC lie in the same range around 800-900°C (2). Due to this fact a thermal integration of exothermic SOFC power generation and endothermic gasification has been studied by a variety of authors (1,3,4).

System concept

Amongst the most promising approaches utilization of the heat generated in the SOFC and post combustion of anode and cathode exhaust can be done by transport of the heat into the gasifier via heat pipes (1,3,4). Compared to a conventional heat pipes based gasifier, where a share of up to 34% (3) of the feedstock is combusted to cover the heat demand, by using heat from the SOFC and post combustion to cover the endothermic gasification process almost the complete feedstock can be gasified, greatly increasing the amount of fuel available for the SOFC. Furthermore the amount of excess air for cooling

of the SOFC to maintain a maximum temperature spread of 100K is reduced to about one third. Consequently the size of the heat exchanger for preheating of cathode air is also reduced significantly.

A further main improvement of the presented system is achieved by integration of a steam cycle. Residual heat of the combustion flue gas below the gasification temperature is used to generate steam at high pressure, which is converted into electricity using a steam turbine. At the same time steam is also needed as gasification agent. Thus, instead of separate steam generation for this purpose, steam is extracted from the steam cycle and fed to the gasifier.

For economic reasons standard wood chips with a high moisture content are used as feedstock for the system. Since a considerable share of the gasification heat demand results from evaporation of feedstock moisture an additional advantage can be gained by partially pre-drying the wood chips. Conventional drying systems use hot air for drying of biomass. However, then the heat of drying is lost. Thus, a more efficient way to dry feedstock is by using the heat of condensation from the steam cycle to dry the wood in pure steam atmosphere, because the steam extracted from the wood can afterwards be condensed and the full amount of heat for drying can be further used for district heating purposes.

Methodology and simulation

All thermodynamic simulations are carried out utilizing the simulation tool Aspen Plus 8.6. Heat integration is done using a pinch analysis approach. The SOFC model used in this work has been developed jointly with partners of the FCH-JU project SOFCOM and has been described previously (5). The gasifier utilized in this work is based on the Heat Pipe Reformer (HPR) concept developed at the Munich Technical University (1) and commercialized by the company Agnion Energy GmbH with currently one unit running in Achenal, Germany. The gas composition, which is typical for this type of gasifier (2), is shown in TABLE I.

TABLE I. Product gas composition.

Compound	Value	Unit
H ₂ O (wet)	39.6	% _{mol}
H ₂ (dry)	53.5	% _{mol}
N ₂ (dry)	2.0	% _{mol}
CO (dry)	13.9	% _{mol}
CO ₂ (dry)	19.3	% _{mol}
CH ₄ (dry)	9.9	% _{mol}
C _x H _y O _z (dry, sum)	1.4	% _{mol}
Trace contaminants		
NH ₃	8.5	ppm
H ₂ S	10,5	ppm
HCl	3,2	ppm
COS	1,9	ppm

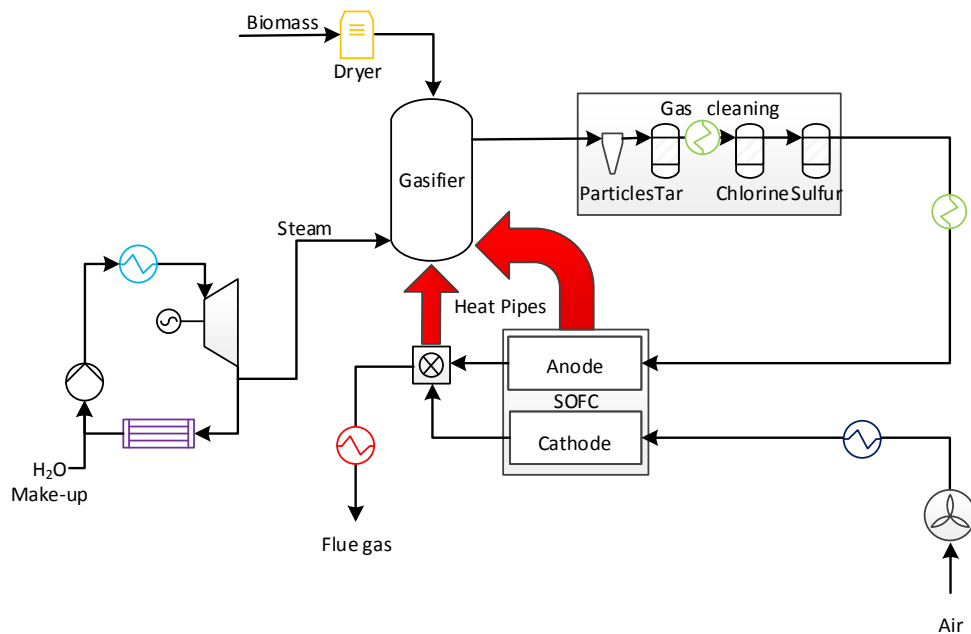


Figure 1. Schematic diagram of the integrated SOFC heat pipe gasifier system. Heat exchanger colors refer to the same colors as shown in Figure 2.

A schematic diagram of the system layout is shown in Figure 1 and relevant parameters for the simulation are shown in TABLE II. Wood chips at a moisture content of 50% are fed to a dryer, where the moisture is reduced to 30%. Then the wood is fed to a fluidized bed gasifier, where it is gasified at 1123K by means of steam acting as fluidization and gasification agent, and heat delivered by heat pipes. A share of 10% of the total carbon input is set as inert and separated from the product gas with a cyclone together with other coarse particles and bed material. Then tars are catalytically cracked using a Dolomite and Nickel based catalyst. After the cracking process the temperature of the product gas is reduced to 573K and in subsequent steps fine particles are filtered using a baghouse filter (not shown), and Chlorine and Sulphur compounds are removed with Potassium carbonate and Zink oxide adsorbents similar to processes described in the literature (6).

Following the cleaning section the product gas is re-heated and fed to the SOFC anode. Here it is converted at a global fuel utilization of 85%, with an anode side internal recirculation rate of 50%. A half of the heat demand of the gasifier is transported directly from the SOFC to the gasifier with heat pipes integrated into the SOFC. Furthermore cathode and anode exhaust are post-combusted together with the inert carbon from the gasifier in a fluidized bed combustion chamber to cover the residual half of the heat demand. The latent heat of the combustion flue gas is used to pre-heat cathode air and produce live steam for the steam turbine, from which then in turn extraction steam is sent to the gasifier.

TABLE II. Parameters chosen for the simulation.

Parameter	Value	Unit
Biomass thermal input (LHV)	8000	kW
Biomass moisture before drying	50	%
Biomass moisture after drying	37.5	%
Gasifier temperature	1123	K
Gasifier pressure drop	0.15	bara
Gasifier outlet pressure	1.25	bara
Heat losses in the gasifier (of biomass LHV)	2.9	%
Charcoal to combustor (share of total carbon input)	10	%
Steam to dry biomass ratio	1.2	kg/kg
Gas cleaning high temperature	1123	K
Gas cleaning low temperature	573	K
SOFC operating voltage	0.8	V
SOFC operating temperature	1123 - 1223	K
SOFC operating pressure	1.025	bara
SOFC anode recirculation ratio	50	%
SOFC global fuel utilization	85	%
SOFC heat loss (based on product gas LHV)	1.0	%
Heat transferred from the SOFC	1873	kW
Heat transferred from the post combustion	1835	kW
Total heat transferred via heat pipes	3708	kW
Steam turbine inlet pressure	99.7	bara
Steam turbine outlet pressure	3.2	bara
Isentropic efficiency (global)	80	%
Mechanical efficiency (global)	90	%
Pressure losses in major heat exchangers	0.02 – 0.05	bara
Inverter efficiency	95	%

Results

Figure 2 shows the Q-T diagram of the system. Colors for specific heat exchangers chosen in the figure are identical to those in Figure 1. As can be seen the combustion flue gas heat exchanger is split in two parts at a flue gas temperature of 930K and a share of about 40% of the flue gas heat is used to generate steam. The split temperature is chosen in order to allow a maximum temperature spread for the high temperature section of the heat exchanger, so that the necessary heat exchanger area with expensive high temperature cladding is minimized. Consequently the pinch point of the steam cycle is extended along the complete steam cycle economizer section.

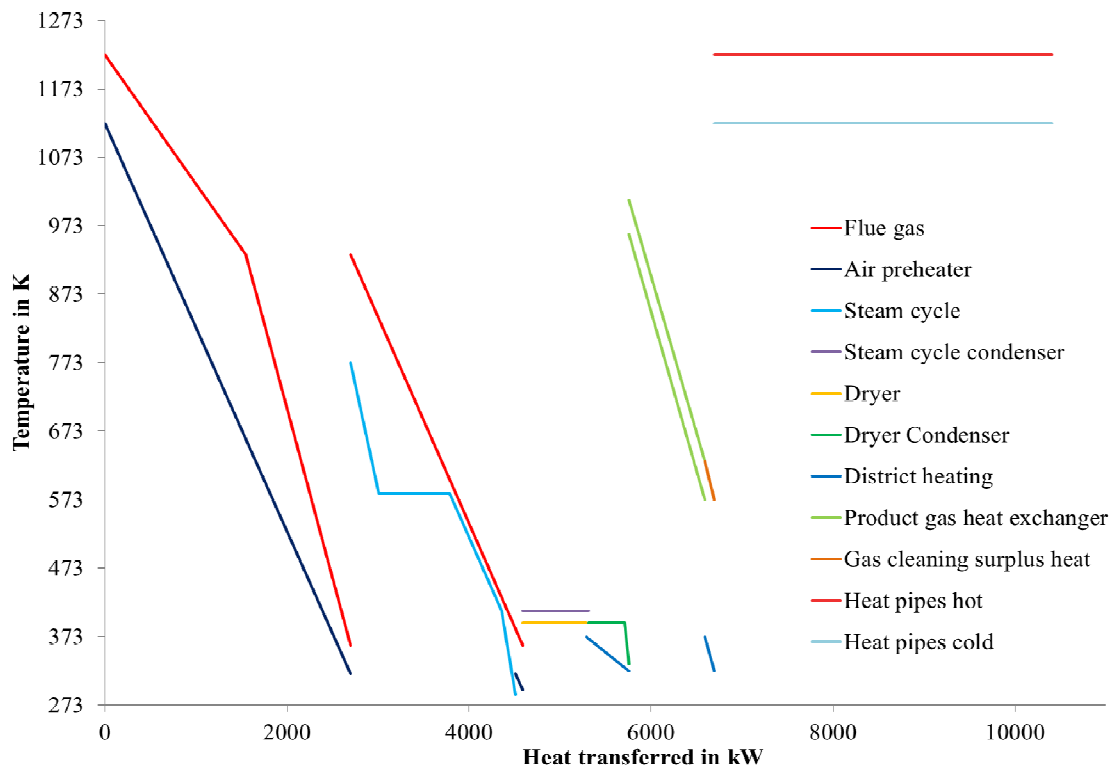


Figure 2. Q-T diagram of the integrated system. The colors are chosen identical to those in Figure 1, additionally district heating and gas cleaning surplus heat are shown, which are not resembled in Figure 1.

As described previously the heat of condensation from the steam turbine exhaust is mostly used for drying of wood chips and the residual heat of condensation is then used for district heating. District heating supply temperature is set to 373K and return temperature to 323K. The product gas mainly exchanges heat with itself inside the gas cleaning section, only a small share of surplus heat is removed also for district heating purposes. Finally the heat pipes evaporation and condensation process is also shown.

TABLE III. Main simulation results.

Stream	Value	Unit
Energy in (LHV)	8000	kW
Exergy in	9399	kW
SOFC power (DC)	4844	kW
SOFC power (AC)	4602	kW
Steam turbine power (AC)	328	kW
Auxiliary consumption (air and recirculation blowers, pumps)	35	kW
Electricity out (net, AC)	4895	kW
District heating	580	kW
Electrical efficiency (LHV)	61.2	%
Thermal efficiency (LHV)	7.3	%
Global efficiency	68.5	%
Exergy efficiency	53.5	%

The key figures of the simulation are summarized in TABLE III. An energy balance, as well as an exergy balance have been performed. Despite the SOFC internal electrical efficiency only being 49.9% of the product gas chemical energy, the system energy balance yields an electrical efficiency of 61.2%. Additionally a thermal efficiency of 7.3%, which leads to a global efficiency of 68.5% based on biomass Lower Heating Value (LHV). Considering the exergy balance, since the initial exergy content of wood calculated according to (7) is far higher than the LHV the overall exergy efficiency is only 53.5%.

Conclusions

In this work a woody biomass based CHP system has been presented. As a result of rigorous heat integration and optimization, especially extracting heat directly from the SOFC to cover the gasification heat demand by means of heat pipes, the electrical efficiency is as high as 61.2%. This is achieved even without pressurization of the SOFC and with comparably small high temperature heat exchangers due to low cooling air flows. However, only a low thermal energy output is obtained, which is mainly attributed to the high steam content in the product gas and consequently the flue gas. Since heat extraction from the flue gas is stopped at 363K before condensation of the steam content starts the latent heat of the flue gas steam content cannot be accessed. If condensation would be allowed the thermal efficiency could be increased, however, acid formation from flue gas components would have to be considered.

Future work will focus on economic evaluation and optimization of the system.

Acknowledgments

The financial support from FCH-JU JTI SOFCOM GA.278798 is gratefully acknowledged.

Furthermore the authors thankfully appreciate the work of several students contributing to the results of this work, especially naming Nicolas Back, and Sebastian Jell.

References

1. K.D. Panopoulos et al., *J. Power Sources*, **159**, 586-594 (2006).
2. M. Mayerhofer et. al., *Fuel*, **99**, 204-209 (2012).
3. S. Karellas et al, *Energy*, **33** (2), 284-291 (2008).
4. P.V. Aravind et al., *Int. J. Renewable Energy Development*, **1**(2), 51-55 (2012).
5. B. Tjaden et al., *Energy & Fuels*, **28**, 4216-4232 (2014).
6. P.V. Aravind and Wiebren de Jong, *Progr. Energy Comb. Sc.*, **38**, 737-764 (2012).
7. G. Song et al., *Energy*, **40**, 164-173 (2012).